THE JOURNAL OF PHYSICAL CHEMISTRY A

Article

pubs.acs.org/JPCA

Including Thermal Disorder of Hydrogen Bonding to Describe the Vibrational Circular Dichroism Spectrum of Zwitterionic L-Alanine in Water

Ednilsom Orestes,[†] Carlos Bistafa,[‡] Roberto Rivelino,[‡,§] and Sylvio Canuto*[,‡]

[†]Instituto de Química, Universidade Federal Fluminense Campus do Valonguinho, CEP 24020-141, Niterói, RJ, Brazil

[‡]Instituto de Física, Universidade de São Paulo, CP 66318, 05914-370 São Paulo, SP, Brazil

[§]Instituto de Física, Universidade Federal da Bahia, 40210-340 Salvador, BA, Brazil

ABSTRACT: The vibrational circular dichroism (VCD) spectrum of L-alanine amino acid in aqueous solution in ambient conditions has been studied. The emphasis has been placed on the inclusion of the thermal disorder of the solute−solvent hydrogen bonds that characterize the aqueous solution condition. A combined and sequential use of molecular mechanics and quantum mechanics was adopted. To calculate the average VCD spectrum, the DFT B3LYP/6-311++G(d,p) level of calculation was employed, over one-hundred configurations composed of the solute plus all water molecules making hydrogen bonds with the solute. Simplified considerations including only four explicit solvent molecules and the polarizable continuum model were also made for comparison. Considering the large number of vibration frequencies with only limited experimental results a direct comparison is presented, when possible, and in addition a statistical analysis of the calculated values was performed. The results are found to be in line with the experiment, leading to the conclusion that including thermal disorder may improve the agreement of the vibrational frequencies with experimental results, but the thermal effects may be of greater value in the calculations of the rotational strengths.

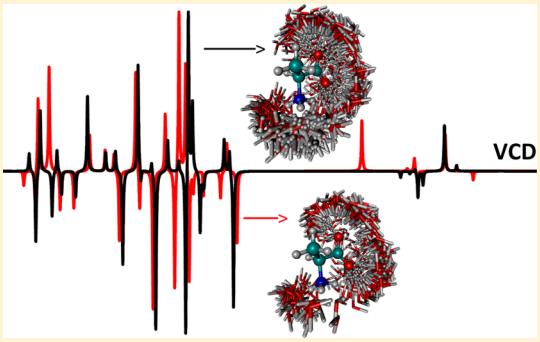

1. INTRODUCTION

The vibrational circular dichroism (VCD) spectroscopy[1,2] has long been recognized as an efficient technique to determine the structure and conformations of chiral molecules of biological interest. Defined as the differential absorption between left and right circularly polarized infrared light by chiral molecules,[3,4] VCD combines the versatility of the vibrational spectroscopy with the stereochemical sensitivity of the optical activity.[5] Among the molecules of interest for calculations of VCD, amino acids have attracted great attention because of their important role in building peptides and proteins, as well as their relatively small size in comparison to the sizes of common biomolecules. Except glycine, all other amino acids are chiral. For this reason, theoretical advances on VCD spectra have been performed by studying the conformations of several chiral molecules.[6−13] However, in such studies the role played by the environment may be crucial to understand the biochemical behavior of these chiral organic compounds. Indeed, to take into account the effects of a biological medium most of the theoretical investigations have to consider a representation of the aqueous environment around the system of interest. Theoretically, this issue has been a great challenge because VCD requires electronic structure calculations and determination of the force field and atomic axial and polar tensors of the molecule in a solvent environment.

Theoretical VCD studies of amino acids have appeared soon after the development of the VCD technique,[14] but neglecting the environmental effects, which can cause large discrepancies between experimental and theoretical results, mainly for biologically relevant polar molecules.[15] For example, the medium influence has been more evident when specific solvent−solute interactions are present, such as hydrogen bonding (HB) formation that is responsible for the internal proton transfer in some amino acids, resulting in a zwitterionic specie.[16−18] Even in the absence of HB, the inclusion of interactions between the solute and the entire first solvation shell, as well as the bulk solvent molecules, may be necessary in some cases.[19] Including the solvent effects along with VCD calculations, however, requires not only a treatment of a significant number of amino acid conformations, which are separated by low energy barriers, but also a significant number of solvent molecules necessary to effectively model the solvent effect.[16] Therefore, despite their relatively small size, solvated amino acids still constitute a challenging problem for theoretical studies aiming at including solvent effects in the VCD spectra.[6]

Special Issue: Jacopo Tomasi Festschrift

Received: August 13, 2014
Revised: November 25, 2014
Published: November 26, 2014

   dx.doi.org/10.1021/jp508205k | J. Phys. Chem. A 2015, 119, 5099−5106

Generally, the method of choice to include the solvent effects around a single molecule is the polarizable continuum model (PCM),[20−22] which is computationally inexpensive and largely adopted currently. However, though implicit solvation, such as PCM and other related models,[23] can be adequate to obtain different properties,[24] explicit solvation is required when the property of interest is directly related with the specific solute−solvent interactions, responsible for important structural changes.[16] This affects the VCD spectra of amino acids, as well as other chiral molecules, in aqueous solution. In this direction, the standard approach to include solvent effects in the VCD spectrum is the microsolvation model.[8,12,16,17,25−28] In this case, few solvent molecules are included in the calculation, near the sites that are amenable to the formation of HB. Constrained optimization of clusters have been also suggested.[29] Additionally, a dielectric continuum model may be employed to describe the medium bulk effects. Thus, the optimized geometries of small clusters are commonly utilized to determine vibrational frequencies and rotational strengths of the system. This has largely been employed to access the VCD spectra of solvated chiral molecules.[8,12,16,17,25−28] A justification of the use of microsolvation in VCD studies is that it is more sensitive to the local environment, with minor influence of the outer solvent molecules around the solute.

In turn, the microsolvation model may have some important limitations: (i) geometry optimizations lead to only one minimum energy structure corresponding to very small temperatures, neglecting the thermal fluctuations of the solvent and hiding the true nature of the liquid, which should be represented by several accessible configurations statistically determined by the thermodynamic conditions. (ii) The choice of the specific sites amenable to bind the solvent molecules and the number of HB are based on chemical intuition, which can influence the calculated properties. For instance, in the case of the calculated VCD spectra changes in the sign of the rotational strength can be obtained, depending on the water distribution around the chiral molecule.[17] In this sense, some works have used QM/MM methods to improve the results.[30−33]

In this work we are interested in analyzing the influence of the thermal disorder of the solute−solvent hydrogen bonds[34,35] in the VCD spectra of amino acids (L-alanine) in water. Opposite to a fixed hydrogen-bond structure (in a minimum-energy condition, or not), in the aqueous environment one must consider the proper thermodynamic condition and therefore the natural disorder of the liquid. Therefore, the proton-acceptor site of a solute molecule in an aqueous environment experiences local thermal disorder that affects the vibrational motion. This disorder has been overlooked in previous theoretical studies of VCD spectra and it is one of our interests here to analyze it in some detail.

We employ the sequential quantum mechanics/molecular mechanics (S-QM/MM)[36] scheme to overcome these limitations and include the thermodynamics effects in the calculated VCD spectrum. The S-QM/MM has successfully been utilized in the calculations of UV−vis spectra,[37−41] NMR constants,[42,43] and excited states.[44,45] In our S-QM/MM approach, the MM calculations are carried out via Monte Carlo (MC) simulations,[46] which generate proper configurations of the solvated system for subsequent QM calculations.[36] In the present purpose, our VCD calculations are performed within density functional theory (DFT).[47]

We compute the VCD spectrum of the zwitterionic L-alanine (zw-L-Ala) amino acid in an aqueous solution under ambient conditions. L-Alanine was selected because it is the smallest naturally occurring chiral amino acid, being present in the primary structure of several proteins. Furthermore, because its zwitterionic form is recognized to be more stable in aqueous solution, giving rise to only one conformer,[16−18] it is a suitable solute for the present study. Our QM solvated amino acid model is, hence, the zw-L-Ala structure embedded in several statistically uncorrelated configurations of water molecules making HB with the solute. In this, we take into account the thermal fluctuations of the solvent around the amino acid. Consequently, these effects are present in the VCD calculations, from which we obtain the corresponding average spectrum of the solvated zw-L-Ala species. For comparison, we also consider calculations using the PCM solvation. Our results for the VCD spectrum are statistically analyzed and compared with available experimental data, as well as with other previous theoretical calculations[17] based on successful microsolvation models.

2. METHODS AND COMPUTATIONAL DETAILS

In the aqueous solution, the zwitterionic form (illustrated in Figure 1) is the most stable structure of L-alanine. Contrary to the neutral form of L-alanine, zw-L-Ala presents just one stable conformer.[16−18] The zw-L-Ala geometry was optimized along with harmonic frequency calculations by employing density functional theory (DFT)[47] methods. As is well-accepted for this system,[16,17,25] we have employed the Becke three-parameter hybrid functional for exchange energy[48] combined with the Lee−Yang−Parr functional for correlation[49] (B3LYP) and calculations were carried out with the 6-311++G(d,p) basis set as implemented in the Gaussian 09 package.[50] The geometry in the water environment was obtained using the PCM[20−22] representation of the solvent. This optimized structure of the zw-L-Ala was then used in the MM part of the sequential QM/MM calculation.[36] As extensively discussed elsewhere,[36,51] this method is a variation of the traditional QM/MM,[52,53] where statistically uncorrelated configurations from the MM partitioning are selected and used in the QM calculations.

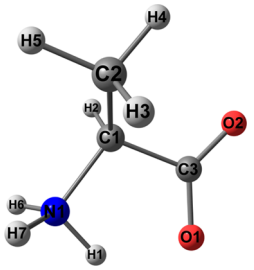

Figure 1. Illustration of the optimized zwitterionic L-alanine (zw-L-Ala) molecule, obtained using PCM at the B3LYP/6-311++G(d,p) level. The labels are used along the text and in other figures.

In the classical partitioning of S-QM/MM, a Monte Carlo Metropolis simulation (MC) was performed, at 25 °C and 1 atm, using the DICE code.[54] The system, composed of one zw-L-Ala species surrounded by 500 water molecules, was simulated in a cubic box with periodic boundary conditions. After thermalization, a simulation of 3.5×10^6 steps/molecule in the isothermal−isobaric (*NPT*) ensemble was performed. The intermolecular interaction was treated using Lennard-Jones (LJ) plus Coulomb potential. The water molecules were modeled by the TIP3P potential.[55] For zw-L-Ala, we have

dx.doi.org/10.1021/jp508205k | J. Phys. Chem. A 2015, 119, 5099−5106

adopted the optimized potentials for liquid simulation-all atoms (OPLS-AA) force field[56] with atomic charges obtained by using the charges from electrostatic potentials using a grid based method (CHELPG),[57] calculated with second order Møller–Plesset perturbation theory (MP2) with the aug-cc-pVDZ basis set, as implemented in the Gaussian 09 package. The present level of calculation provides a good compromise between performance and accuracy to describe charges and dipole moments.[58] To include the electronic polarization effects, both geometry and charges were obtained considering the zw-L-Ala in aqueous environment, using the PCM representation of the solvent.

As in previous works,[37−41] we used the autocorrelation function of the energy[36,46] to select 100 uncorrelated solute–solvent configurations from the MC simulation, with less than 10% of statistical correlation. All of these solute–solvent configurations are employed in the quantum mechanical calculations at the DFT level. Before performing these DFT calculations, we have carefully identified the hydrogen bonds using the energetic and geometric criteria,[35,59,60] and this will be detailed in the following section. During the DFT calculations, only the water molecules satisfying the HB criteria are included. For the calculation of the vibration frequencies and the VCD spectrum of zw-L-Ala without including the frequencies of the water molecules, only the geometry of the solute zw-L-Ala was re-optimized in the presence of the HB water molecules that are kept fixed. This gives the separated spectrum of zw-L-Ala and preserves the thermal disorder associated with the thermodynamic distribution of the solvent molecules as obtained from the simulation. To determine the VCD intensities, atomic polar and axial tensors were calculated using analytical derivative methods. The electronic properties were obtained as simple averages over the calculations for each configuration.

3. RESULTS AND DISCUSSION

Statistical Analysis of the Solute–Solvent Hydrogen Bonds. Hydrogen bonds are normally characterized by the appropriate angular distribution and the pairwise radial distribution function. Although this gives the coordination of solvent molecules around a certain atom of the solute, it cannot be assured that all neighboring solvent molecules are indeed hydrogen bonded to the solute. In addition, to these geometric criteria it is important to add an energetic condition.[35,59,60] Figure 2 shows the pairwise radial distribution functions, $G(r)$ needed for analyzing the solute–solvent hydrogen bonds. In Figure 2a we show, for instance the distribution between the two oxygen atoms of zw-L-Ala and the hydrogen atom of water. For the oxygen atom, termed as O1, Figure 1, we clearly note a first peak in the G_{O1-Ow} starting at 2.3 Å and ending at 3.2 Å. These define the first hydration shell around O1. Integration of this peak gives, on average, 2.5 water molecules around the O1 atom. Similar results are also shown for the other oxygen atom as well as the nitrogen atom. For instance, the first peaks of G_{O2-Ow} and G_{N1-Ow} end in 3.2 and 3.5 Å, respectively. Analysis of these peaks gives, on average, 3.1 and 3.9 water molecules coordinating with O2 and NH_x (x = 1, 2, 3), respectively, Figure 1. Hence, the geometric criteria adopted for a solute–solvent HB is R_{O-Ow} or R_{N-Ow} < 3.5 Å and the angle $\theta_{O-(OH)w}$ < 40° or θ_{NH-Ow} < 40°.

The energetic criterion was established by analyzing the histogram of the pairwise interaction energy between zw-L-Ala and the water molecules, displayed in Figure 3. The first bump

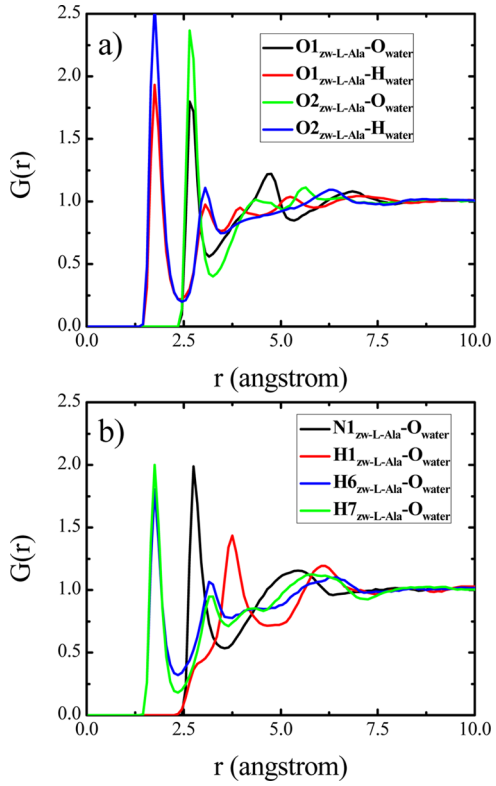

Figure 2. Calculated $G(r)$: (a) between the zw-L-Ala oxygen atoms and water hydrogen atoms; (b) between the zw-L-Ala NH_3^+ group and water oxygen atoms. See atomic labels in Figure 1.

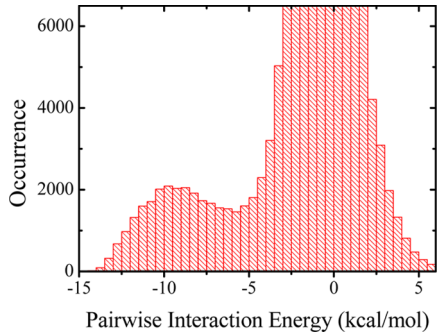

Figure 3. Distribution of pairwise interaction energy between zw-L-Ala and water.

corresponding to the HBs exhibits a minimum around −5.5 kcal/mol. The energetic condition is thus that the interaction energy between water zw-L-Ala is at least −5.5 kcal/mol.

Using both geometric and energetic criteria, we find the distribution of the numbers of hydrogen bonds ranging from a minimum of 5 water molecules and a maximum of 9. Figure 4a illustrates the configuration space occupied by these hydrogen bonds by showing a superposition of all these configurations with water molecules hydrogen bonded to zw-L-Ala. On the average we obtain 7 water molecules that are hydrogen bonded to zw-L-Ala. There are 2.3 HB in the O1, 2.6 in the O2, and 2.1 in the NH_x sites. These numbers are summarized in Table 1. Using the angular distribution, it is possible to discern the three NH_x possibilities and in more detail: on average we find 0.13 HBs around N1H1, 1.01 around N1H6, and 0.99 around N1H7. The small number of hydrogen bonds in the N1H1 site is an indication of some steric effect but more likely that H1

dx.doi.org/10.1021/jp508205k | J. Phys. Chem. A 2015, 119, 5099–5106

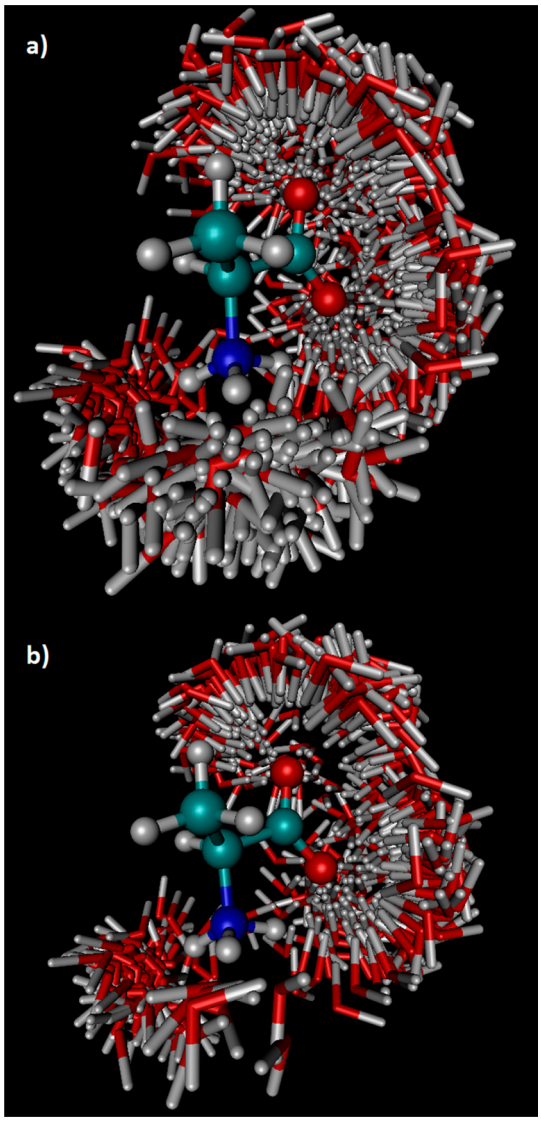

Figure 4. Illustration of the configuration space spanned by all the water molecules that are hydrogen bonded to HB zw-L-Ala as obtained from the MC simulation. In (b) only four water molecules are considered. This figure was constructed using the VMD program.[61]

Table 1. Distribution of Water Molecules around the Sites Amenable to Hydrogen Bonds

	O1	O2	NHx
coordination no.[a]	2.5	3.1	3.9
no. of hydrogen bonds[b]	2.3	2.6	2.1

[a]Integration of the first peak of the radial distribution function. [b]Obtained using the geometric and energetic criterion (see text).

makes an intramolecular hydrogen bond with the O1 atom of zw-L-Ala. Indeed, this can be noted by the absence of an intermolecular hydrogen bond shell in the G_{H1-Ow} (red curve in Figure 2b), distribution.

In microsolvation studies four water molecules are normally considered in optimized clusters of alanine.[17,25] Thus, in addition, for comparison, we have also calculated the VCD spectrum using another set of calculations with only the 4 nearest water molecules forming HB. We constrain in this case, three water molecules around the COO^- group and one around the NH_3^+ group. These configurations are illustrated in Figure 4b. The first case is termed as "zw-L-$Ala_{re\text{-}opt}$ + all $HB_{average}$" and the second as "zw-L-$Ala_{re\text{-}opt}$ + 4 $HB_{average}$". In the first, in each configuration the number of water molecules varies between five and nine. In the second the number of water molecules is fixed to four and are extracted from the simulation, thus also including thermal disorder.

To obtain the spectrum, the calculated vibrational rotational strengths are averaged over the 100 configurations. The subscript "re-opt" in zw-L-Ala means that the solute molecular structure was relaxed in the presence of the solvent and the subscript "average" denotes that the results are obtained as average of 100 configurations generated in the MC simulation.

Analysis of the Calculated VCD Spectrum. Now we discuss the results obtained with two statistically oriented models and compare with the simple PCM approach and the previous microsolvation study. Jalkanen et al.[18] have compared microsolvation models (optimized clusters) of zw-L-Ala + 9 H_2O and zw-L-Ala +20 H_2O (corresponding to the entire first solvation shell) and found mild differences in the calculated VCD spectra. Indeed, the inclusion of additional water molecules beyond those forming HB produces no significant effects in the VCD spectrum of zw-L-Ala. For this reason, we have first computed the vibrational rotation strengths considering all statistically uncorrelated configurations containing the hydrated zw-L-Ala species satisfying the HB criteria, i.e., employing our "zw-L-$Ala_{re\text{-}opt}$ + all $HB_{average}$" model. The calculated frequencies and VCD intensities are reported in Table 2. Other works using the microsolvation model for zw-L-Ala have adopted four water molecules to represent the possible HB with the solvent.[17,25] Table 2 also shows our results obtained using the simpler PCM and the same B3LYP/6-311++G(d,p) level. The experimental vibrational frequencies were determined in the work of Diem et al.,[62] and the microsolvation results were carried out by Frimand et al.[17] that used an optimized cluster of zw-L-Ala + 9 H_2O combined with the reaction field of Onsager and the B3LYP/6-31G(d) level of theory. They have shown that nine hydrogen-bonded water molecules around zw-L-Ala, along with the Onsager model essentially gives the entire solvent effect in the VCD spectrum.

In the high-frequency side our theoretical results are overestimated compared to experimental results, as expected. For proper comparison we should mention that our results in Table 2 were not rescaled by convenient but arbitrary factors.[63,64] In the intermediate and more interesting spectral region ranging from 1100 to 1460 cm^{-1} two experimental results are available for comparison. The lowest frequency observed at 1110−1117 cm^{-1}, assigned to the ν^{as}(CCN) mode of the $CH_3-C-NH_3^+$ group, is well described by all theoretical methods considered and it can be noted that the zw-L-$Ala_{re\text{-}opt}$ + all $HB_{average}$ is in agreement with experiment. Similarly for the highest frequency observed at 1459−1471 cm^{-1}, assigned to the $\delta^{as}(-CH_3)$ mode, the zw-L-$Ala_{re\text{-}opt}$ + all $HB_{average}$ result is 1478 cm^{-1}. The analysis of the vibrational mode of a molecule in solution is not always simple because closely lying transitions may interchange position in different configurations. For example, in a selected configuration the frequency of the $\nu^s(NH_3^+)$ symmetric stretch mode is only slightly larger than the asymmetric stretch $\nu^{as}(NH_3^+)$ and may interchange in different configurations. Moreover, the sign of the VCD intensity can appear inverted for specific vibrational modes and strongly depends on the local environment. This inversion can also be obtained in different optimized clusters commonly used in microsolvation models.[17] In a liquid situation, the

dx.doi.org/10.1021/jp508205k | J. Phys. Chem. A 2015, 119, 5099−5106

Table 2. Calculated VCD Spectrum of zw-L-Ala in Water, Using B3LYP/6-311++G(d,p)[a]

Frimand et al.[b]		zw-l-Ala + PCM		zw-L-Ala$_{re\text{-}opt}$ + 4HB$_{average}$		zw-l-Ala$_{re\text{-}opt}$ + all HB$_{average}$		exp[c]	
freq	RS	freq	RS	freq	RS	freq	RS	freq	$A\varepsilon/\varepsilon$[d]
3161	3	3543	−1	3525	−6	3400	3	3080	
3138	−14	3482	13	3315	23	3310	20	3060	
3103	−8	3135	2	3137	0	3149	−6	3020	
3086	−24	3113	−27	3106	−9	3111	−12	3003	
3066	17	3096	19	3084	8	3086	1	2993	
3026	40	3037	1	3030	2	3050	−1	2962	
2990	17	3030	−30	2690	31	2981	−3	2949	
1778	14	1665	−19	1754	−45	1728	−61	1645	
1766	−17	1654	−75	1678	18	1697	10	1625	
1678	−65	1632	19	1630	−17	1657	14	1607	
1653	−26	1492	−20	1502	−16	1507	−6	1498	
1536	0	1489	5	1492	2	1497	−6	1459	
1529	−14	1426	−22	1427	−13	1478	−27	1459, 1471[d]	
1456	77	1404	38	1396	−71	1420	30	1410, 1418[d]	5.2
1422	21	1374	74	1368	69	1389	75	1375, 1381[d]	
1394	−171	1349	−27	1319	100	1369	−77	1351, 1358[d]	−27
1351	99	1306	−11	1287	−75	1317	5	1301, 1306[d]	16
1274	14	1210	14	1216	36	1234	14	1220, 1221[d]	5.3
1207	4	1114	−71	1124	−86	1145	−70	1145, 1139[d]	−4.2
1143	−10	1092	14	1089	1	1114	5	1110, 1117[d]	−4.7
1057	12	996	−43	1024	−25	1033	−6	1001	
1030	−7	990	67	994	62	1012	48	995	
938	−19	875	−46	872	−44	898	−42	922	
854	18	822	3	831	11	843	9	850	
771	−3	764	24	765	13	770	8	775	
704	4	624	31	649	22	633	33	640	
632	29	517	−17	531	−23	544	−12	527	
533	6	393	4	428	−24	439	−10	477	
436	−12	334	29	391	0	404	10	399	
363	−35	266	26	345	65	368	−20	296	
291	37	247	−36	262	46	279	28	283	
262	−28	239	−39	240	−20	245	−32	219	
152	−1	44	−0.5	155	−9	195	8	184	

[a]Frequencies in cm^{-1} and rotational strength in 10^{-44} esu^2 cm^2. Also presented are the experimental VCD intensities in terms of molar extinction coefficients ($\Delta\varepsilon/\varepsilon$) in L/(mol cm), related to the rotational strength through the integration of the peak. [b]zw-L-Ala +9H_2O + Onsager, at the B3LYP/6-31G* level, calculated in ref 17. [c]Reference 62. [d]Reference 65.

experimental VCD spectra will not correspond to an optimized configuration, but to an average over several configurations, and it is important to be able to capture this thermal effect of the solvent.

To have a better overall comparison between the different theoretical methods, we show in Table 3 the corresponding statistical parameters for comparing the accuracy. We have considered the root-mean-square deviation (RMSD), the mean accumulated deviation (MAD), and the mean absolute percentage error (MAPE), defined below

$$\mathrm{RMSD}(f^{\mathrm{calc}} f^{\mathrm{exp}}) = \sqrt{\frac{\sum_i (f_i^{\mathrm{calc}} - f_i^{\mathrm{exp}})^2}{n_{\mathrm{freq}}}} \quad (1)$$

$$\mathrm{MAD}(f^{\mathrm{calc}} f^{\mathrm{exp}}) = \frac{\sum_i |f_i^{\mathrm{calc}} - f_i^{\mathrm{exp}}|}{n_{\mathrm{freq}}} \quad (2)$$

$$\mathrm{MAPE}(f^{\mathrm{calc}} f^{\mathrm{exp}}) = \frac{1}{n_{\mathrm{freq}}} \sum_i \frac{|f_i^{\mathrm{calc}} - f_i^{\mathrm{exp}}|}{f_i^{\mathrm{calc}}} \quad (3)$$

In all of the above equations, f^{calc} and f^{exp} are, respectively, the calculated and experimental vibrational frequencies, and n_{freq} is the total number of vibrational modes. From the analysis of RMSD, MAD, and MAP (Table 3) we can evaluate the performance of each method. The frequencies calculated using PCM are only in a reasonable agreement with the experimental values. The frequencies calculated by Frimand et al.[17] using a microsolvation model represent an improvement in comparison with the PCM results by including structural effects of the

Table 3. Root Mean Square Deviation (RMSD), Mean Accumulated Deviation (MAD), and Mean Absolute Percentage Error (MAPE)

	RMSD	MAD	MAPE
Frimand et al.[a]	70.3	61.0	5.92
zw-L-Ala + PCM	120.9	63.0	14.08
zw-L-Ala$_{re\text{-}opt}$ + 4 HB$_{average}$	109.8	60.5	4.34
zw-L-Ala$_{re\text{-}opt}$ + all HB$_{average}$	84.9	49.5	3.48

[a]zw-L-Ala +9H_2O + Onsager, at the B3LYP/6-31G* level, calculated in ref 17.

dx.doi.org/10.1021/jp508205k | J. Phys. Chem. A 2015, 119, 5099−5106

solvent. We note a considerable reduction of the statistical errors, specially the mean average percentage error. Considering now the two models including the thermal disorder of the hydrogen-bonded water molecules, an even better agreement is achieved. We obtain, however, a larger RMSD value, as compared to the microsolvation model because, as discussed above, our calculated higher frequencies are overestimated compared to the experimental values. In the microsolvation model all molecules hydrogen-bonded to the solute are also optimized, but the thermal disorder is entirely neglected. The highest frequencies of the microsolvated system tend to be shifted to lower values.

Our results support the findings[17,18] that the inclusion of the HB water molecules is enough to account for the solvent effects in the VCD frequencies of the zw-L-Ala in aqueous solution. In complement, our results also emphasize the importance of the inclusion of thermodynamic conditions in this study. For example, using our model containing only four HB with the solute (zw-L-$Ala_{re\text{-}opt}$ + 4 $HB_{average}$), we obtain a better agreement with experimental values than the previous work, which used nine H_2O molecules around zw-L-Ala.

Figure 5 shows the calculated VCD spectrum obtained from a convolution using a Lorentzian function around the individual

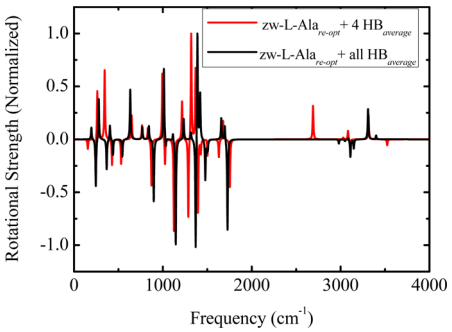

Figure 5. Convoluted average VCD spectra of zw-L-Ala in water using the average frequencies and intensities values. A Lorentzian function with a half-width of 5 cm^{-1} was used.

average frequencies and rotational strengths with an arbitrary half-width of 5 cm^{-1}. This compares favorably with the experimental spectrum[62,65] (see also ref 17).

We now discuss the rotational strength of some individual modes. For zw-L-Ala, the VCD intensities of six modes are experimentally well-known.[65] Their values, in terms of molar extinction coefficients [L/(mol cm)], are also shown in Table 2. The comparison is not straightforward (the molar extinction coefficients are related to the rotational strength through the integration of a peak) but gives the correct idea of the intensities and their signs. Regarding the experimental mode at 1418 cm^{-1}, with an intensity of 5.2 L/(mol cm), the theoretical average rotational strength with the zw-L-$Ala_{re\text{-}opt}$ + all $HB_{average}$ model is 30 × 10^{-44} esu^2 cm^2, whereas the zw-L-$Ala_{re\text{-}opt}$ + 4 $HB_{average}$ model presents the rotational strength with opposite signal (−71 × 10^{-44} esu^2 cm^2). The same is observed for the modes at 1351−1358 and 1301−1306 cm^{-1}, where the correct sign is obtained with the zw-L-$Ala_{re\text{-}opt}$ + all $HB_{average}$ model, but an opposite sign is obtained using zw-L-$Ala_{re\text{-}opt}$ + 4 $HB_{average}$. This gives evidence that using a limited number of water molecules can still present good values for the frequencies but may present limitations for the description of the rotational strengths. In particular, those two vibrational modes are mainly related to a bending of H bonded to the chiral C, δ(C*−H), and due to the limited number of water molecules included, the ordering of the modes may be reversed. Of the six rotational strength values known experimentally, the zw-L-$Ala_{re\text{-}opt}$ + all $HB_{average}$ model describe five correctly. It fails only in describing the sign of the rotational strength of the mode measured at 1110−1117 cm^{-1}. For this, also the PCM and the zw-L-$Ala_{re\text{-}opt}$ + 4 $HB_{average}$ model fail, presenting a positive rotational strength, compared with the experimental small but negative value.

In general, the zw-L-$Ala_{re\text{-}opt}$ + 4 $HB_{average}$ does not work in the same fashion as the zw-L-$Ala_{re\text{-}opt}$ + all $HB_{average}$ model in describing the sign of the rotational strength. However, the results of Frimand et al.[17] using nine water molecules with the microsolvation model have a performance that can be considered close to our best model, in describing the sign of the rotational strength. Note that Frimand et al.[17] correctly describe the rotational strength of the vibrational mode at 1110−1117 cm^{-1} but fail in describing the mode measured at 1139 cm^{-1}, whereas all other theoretical models describe it correctly. As has been recognized, improvements are still necessary to accurately describe the rotational strength by using DFT methods.[10] As is known, the rotational strength in VCD is a local property so that the dominant solvent effect depends essentially on the molecules forming HB with the solute.[8,12,16,17,25−28] This is reemphasized from the present results, considering explicit solvent molecules around the solute.

4. CONCLUSIONS

The importance of including the appropriate thermal disorder of HB molecules, associated with the thermodynamic conditions, to accurately describe the solvent effect in the VCD spectrum of solvated molecules has been analyzed. We have considered the theoretical VCD spectrum of the L-alanine in solution, at ambient condition, considering its zwitterionic form. Most studies considering explicit solvent molecules use microsolvation models that are known to eventually present their limitations for the VCD spectra of amino acids in aqueous solution. The emphasis of this study has been placed in including the thermal disorder of the hydrogen bonds and to analyze its effect on the VCD spectrum, including both the vibrational frequencies and the rotational strengths. Thus, we have considered a combined and sequential use of molecular mechanics and quantum mechanics. Monte Carlo simulations were performed to generate the structures composed of alanine and water in normal thermodynamic condition. To evaluate the VCD spectrum, we have employed the DFT B3LYP/6-311++G(d,p) level of calculations for over 100 configurations composed of the solute plus all water molecules making hydrogen bonds with the solute. This relies on the general agreement that solvent water molecules forming hydrogen bonding with the solute dominate the influence of the aqueous medium on the VCD spectrum of the zwitterionic L-alanine.

We have also considered calculations using a smaller number of water molecules and the polarizable continuum model. Including all solvent molecules that make a hydrogen bond with the solute improves the results. Considering the large number of vibrations and the limited access to experimental values available, we present in addition to a direct comparison, when possible, also the statistical analysis of the calculated values. In general the results are found to be in good agreement with experiment with the conclusion that including thermal

dx.doi.org/10.1021/jp508205k | J. Phys. Chem. A 2015, 119, 5099−5106

disorder leads to an overall better agreement with experiment. In general, the results indicate that the thermal effects may be of greater value in the calculations of the rotational strengths.

AUTHOR INFORMATION

Notes

The authors declare no competing financial interest.

ACKNOWLEDGMENTS

This work has been partially supported by FAPESP, CNPq, and CAPES (Brazil).

REFERENCES

(1) Holzwarth, G.; Hsu, E. C.; Mosher, H. S.; Faulkner, T. R.; Moscowitz, A. Infrared Circular Dichroism of Carbon-Hydrogen and Carbon-Deuterium Stretching Modes. Observations. *J. Am. Chem. Soc.* **1974**, *96*, 251−252.

(2) Nafie, L. A.; Keiderling, T. A.; Stephens, P. J. Vibrational Circular Dichroism. *J. Am. Chem. Soc.* **1976**, *98*, 2715−2723.

(3) Nordén, B.; Rodger, A.; Dafforn, T. *Linear Dichroism and Circular Dichroism: A Textbook on Polarized-Light Spectroscopy*; RSC Publishing: London, 2010; p 304.

(4) Ruud, K. Ab Initio Methods for Vibrational Circular Dichroism and Raman Optical Activity. In *Comprehensive Chiroptical Spectroscopy* Vol. *1*; Berova, N., Polavarapu, P. L., Nakanishi, K., Woody, R. W., Eds.; Wiley: Hoboken, NJ, USA, 2012; pp 699−728.

(5) Eliel, E. L.; Wilen, S. H.; Doyle, M. P. *Basic Organic Stereochemistry*; John Wiley & Sons, Inc.: Hoboken, NJ, USA, 2001; p 704.

(6) Freedman, T. B.; Cao, X.; Oliveira, R. V.; Cass, Q. B.; Nafie, L. A. Determination of the Absolute Configuration and Solution Conformation of Gossypol by Vibrational Circuldar Dichroism. *Chirality* **2003**, *15*, 196−200.

(7) Sadlej, J.; Dobrowolski, J. C.; Rode, J. E.; Jamróz, M. H. DFT Study of Vibrational Circular Dichroism Spectra of D-Lactic Acid-Water Complexes. *Phys. Chem. Chem. Phys.* **2006**, *8*, 101−113.

(8) Sadlej, J.; Dobrowolski, J. C.; Rode, J. E.; Jamróz, M. H. Density Functional Theory Study on Vibrational Circular Dichroism as a Tool for Analysis of Intermolecular Systems: (1:1) Cysteine-Water Complex Conformations. *J. Phys. Chem. A* **2007**, *111*, 10703−10711.

(9) Mcconnell, O.; He, Y.; Nogle, L.; Sarkahian, A. N. I. Application of Chiral Technology in a Pharmaceutical Company. Enantiomeric Separation and Spectroscopic Studies of Key Asymmetric Intermediates Using a Combination of Techniques. Phenylglycidols. *Chirality* **2007**, *19*, 716−730.

(10) Sadlej, J.; Dobrowolski, J. C.; Rode, J. E. VCD Spectroscopy as a Novel Probe for Chirality Transfer in Molecular Interactions. *Chem. Soc. Rev.* **2010**, *39*, 1478−1488.

(11) Barone, V.; Baiardi, A.; Biczysko, M.; Bloino, J.; Cappelli, C.; Lipparini, F. Implementation and Validation of a Multi-Purpose Virtual Spectrometer for Large Systems in Complex Environments. *Phys. Chem. Chem. Phys.* **2012**, *14*, 12404.

(12) Rode, J. E.; Dobrowolski, J. C.; Sadlej, J. Prediction of (L)-Methionine VCD Spectra in the Gas Phase and Water Solution. *J. Phys. Chem. B* **2013**, *117*, 14202−14214.

(13) Ganesan, A.; Brunger, M. J.; Wang, F. A Study of Aliphatic Amino Acids Using Simulated Vibrational Circular Dichroism and Raman Optical Activity Spectra. *Eur. Phys. J. D* **2013**, *67*, 229.

(14) Barron, L. D. Theoretical Rayleigh Optical Activity of Hexahelicene. *J. Am. Chem. Soc.* **1974**, *96*, 6761−6762.

(15) Compagnon, I.; Oomens, J.; Meijer, G.; von Helden, G. Mid-Infrared Spectroscopy of Protected Peptides in the Gas Phase: A Probe of the Backbone Conformation. *J. Am. Chem. Soc.* **2006**, *128*, 3592−3597.

(16) Jalkanen, K. J.; Degtyarenko, I. M.; Nieminen, R. M.; Cao, X.; Nafie, L. A.; Zhu, F.; Barron, L. D. Role of Hydration in Determining the Structure and Vibrational Spectra of L-Alanine and N-Acetyl L-Alanine N′-Methylamide in Aqueous Solution: A Combined Theoretical and Experimental Approach. *Theor. Chem. Acc.* **2008**, *119*, 191−210.

(17) Frimand, K.; Bohr, H.; Jalkanen, K. J.; Suhai, S. Structures, Vibrational Absorption and Vibrational Circular Dichroism Spectra of L-Alanine in Aqueous Solution: A Density Functional Theory and RHF Study. *Chem. Phys.* **2000**, *255*, 165−194.

(18) Jalkanen, K. J.; Suhai, S.; Bohr, H. G. Quantum Molecular Biological Methods Using Density Functional Theory. In *Handbook of Molecular Biophysics. Methods and Applications*; Bohr, H. G., Ed.; Wiley-VCH: Weinheim, 2009; pp 7−66.

(19) Müller, T.; Wiberg, K. B.; Vaccaro, P. H. Cavity Ring-Down Polarimetry (CRDP): A New Scheme for Probing Circular Birefringence and Circular Dichroism in the Gas Phase. *J. Phys. Chem. A* **2000**, *104*, 5959−5968.

(20) Tomasi, J.; Persico, M. Molecular Interactions in Solution: An Overview of Methods Based on Continuous Distributions of the Solvent. *Chem. Rev.* **1994**, *1994*, 2027−2094.

(21) Tomasi, J. Thirty Years of Continuum Solvation Chemistry: A Review, and Prospects for the near Future. *Theor. Chem. Acc.* **2004**, *112*, 184−203.

(22) Tomasi, J.; Mennucci, B.; Cammi, R. Quantum Mechanical Continuum Solvation Models. *Chem. Rev.* **2005**, *105*, 2999−3093.

(23) Klamt, A.; Schüürmann, G. COSMO: A New Approach to Dielectric Screening in Solvents with Explicit Expressions for the Screening Energy and Its Gradient. *J. Chem. Soc., Perkin Trans.* **1993**, *2*, 799−805.

(24) Barone, V.; Cossi, M. Quantum Calculation of Molecular Energies and Energy Gradients in Solution by a Conductor Solvent Model. *J. Phys. Chem. A* **1998**, *102*, 1995−2001.

(25) Tajkhorshid, E.; Jalkanen, K. J.; Suhai, S. Structure and Vibrational Spectra of the Zwitterion L-Alanine in the Presence of Explicit Water Molecules: A Density Functional Analysis. *J. Phys. Chem. B* **1998**, *102*, 5899−5913.

(26) Abdali, S.; Jalkanen, K. J.; Bohr, H.; Suhai, S.; Nieminen, R. M. The VA and VCD Spectra of Various Isotopomers of L -Alanine in Aqueous Solution. *Chem. Phys.* **2002**, *282*, 219−235.

(27) Debie, E.; Bultinck, P.; Herrebout, W.; van der Veken, B. Solvent Effects on IR and VCD Spectra of Natural Products: An Experimental and Theoretical VCD Study of Pulegone. *Phys. Chem. Chem. Phys.* **2008**, *10*, 3498−3508.

(28) Zhang, R. bo; Eriksson, L. A. Theoretical Study on Conformational Preferences of Ribose in 2-Thiouridine–the Role of the 2′OH Group. *Phys. Chem. Chem. Phys.* **2010**, *12*, 3690−3697.

(29) Hudecová, J.; Hopmann, K. H.; Bouř, P. Correction of Vibrational Broadening in Molecular Dynamics Clusters with the Normal Mode Optimization Method. *J. Phys. Chem. B* **2012**, *116*, 336−342.

(30) Poopari, M. R.; Dezhahang, Z.; Xu, Y. A Comparative VCD Study of Methyl Mandelate in Methanol, Dimethyl Sulfoxide, and Chloroform: Explicit and Implicit Solvation Models. *Phys. Chem. Chem. Phys.* **2013**, *15*, 1655−1665.

(31) Mukhopadhyay, P.; Zuber, G.; Wipf, P.; Beratan, D. N. Contribution of a Solute's Chiral Solvent Imprint to Optical Rotation. *Angew. Chem. Int. Ed.* **2007**, *46*, 6450−6452.

(32) Kundrat, M. D.; Autschbach, J. Ab Initio and Density Functional Theory Modeling of the Chiroptical Response of Glycine and Alanine in Solution Using Explicit Solvation and Molecular Dynamics. *J. Chem. Theory Comput.* **2008**, *4*, 1902−1914.

(33) Kundrat, M. D.; Autschbach, J. Modeling of the Chiroptical Response of Chiral Amino Acids in Solution Using Explicit Solvation and Molecular Dynamics. *J. Chem. Theory Comput.* **2009**, *5*, 1051−1060.

(34) Malaspina, T.; Coutinho, K.; Canuto, S. Ab Initio Calculation of Hydrogen Bonds in Liquids: A Sequential Monte Carlo Quantum Mechanics Study of Pyridine in Water. *J. Chem. Phys.* **2002**, *117*, 1692−1699.

(35) Fileti, E. E.; Coutinho, K.; Malaspina, T.; Canuto, S. Electronic Changes due to Thermal Disorder of Hydrogen Bonds in Liquids: Pyridine in an Aqueous Environment. *Phys. Rev. E* **2003**, *67*, 061504.
(36) Coutinho, K.; Rivelino, R.; Georg, H. C.; Canuto, S. The Sequential QM/MM Method and Its Applications to Solvent Effects in Electronic and Structural Properties of Solutes. In *Solvation Effects on Molecules and Biomolecules. Computational Methods and Applications*; Canuto, S., Ed.; Springer: Berlin, 2008; pp 159−189.
(37) Ludwig, V.; Coutinho, K.; Canuto, S. Sequential Classical-Quantum Description of the Absorption Spectrum of the Hydrated Electron. *Phys. Rev. B* **2004**, *70*, 214110.
(38) Ludwig, V.; Coutinho, K.; Canuto, S. A Monte Carlo-Quantum Mechanics Study of the Lowest N−π^* and Π−π^* States of Uracil in Water. *Phys. Chem. Chem. Phys.* **2007**, *9*, 4907−4912.
(39) Malaspina, T.; Coutinho, K.; Canuto, S. Analyzing the N-Π* Eletronic Transition of Formaldehyde in Water. A Sequential Monte Carlo/Time-Dependent Density Functional Theory. *J. Brazilian Chem. Soc.* **2008**, *19*, 305−311.
(40) Jaramillo, P.; Coutinho, K.; Cabral, B. J. C.; Canuto, S. Explicit Solvent Effects on the Visible Absorption Spectrum of a Photosynthetic Pigment: Chlorophyll-c2 in Methanol. *Chem. Phys. Lett.* **2011**, *516*, 250−253.
(41) Bistafa, C.; Canuto, S. Solvent Effects on the Two Lowest-Lying Singlet Excited States of 5-Fluorouracil. *Theor. Chem. Acc.* **2013**, *132*, 1299.
(42) Manzoni, V.; Lyra, M. L.; Gester, R. M.; Coutinho, K.; Canuto, S. Study of the Optical and Magnetic Properties of Pyrimidine in Water Combining PCM and QM/MM Methodologies. *Phys. Chem. Chem. Phys.* **2010**, *12*, 14023−14033.
(43) Gester, R. M.; Bistafa, C.; Georg, H. C.; Coutinho, K.; Canuto, S. Theoretically Describing the 17O Magnetic Shielding Constant of Biomolecular Systems: Uracil and 5-Fluorouracil in Water Environment. *Theor. Chem. Acc.* **2014**, *133*, 1424.
(44) Orozco-González, Y.; Coutinho, K.; Canuto, S. Excited State Electronic Polarization and Reappraisal of the N←π^* Emission of Acetone in Water. *Chem. Phys. Lett.* **2010**, *499*, 108−112.
(45) Orozco-Gonzalez, Y.; Bistafa, C.; Canuto, S. Solvent Effect on the Stokes Shift and on the Nonfluorescent Decay of the Daidzein Molecular System. *J. Phys. Chem. A* **2013**, *117*, 4404−4411.
(46) Allen, M. P.; Tildesley, D. J. *Computer Simulation of Liquids*; Oxford University Press: Oxford, U.K., 1987; p 385.
(47) Parr, R. G.; Yang, W. *Density-Functional Theory of Atoms and Molecules*; Oxford Science Publications: New York, 1989.
(48) Becke, A. D. A New Mixing of Hartree−Fock and Local Density-Functional Theories. *J. Chem. Phys.* **1993**, *98*, 1372−1377.
(49) Lee, C.; Yang, W.; Parr, R. G. Development of the Colle-Salvetti Correlation-Energy Formula into a Functional of the Electron Density. *Phys. Rev. B* **1988**, *37*, 785−789.
(50) Frisch, M. J.; Trucks, G. W.; Schlegel, H. B.; Scuseria, G. E.; Robb, M. A.; Cheeseman, J. R.; Scalmani, G.; Barone, V.; Mennucci, B.; Petersson, G. A.; et al. *Gaussian 09*; Gaussian Inc.: Wallingford, CT, 2009.
(51) Coutinho, K.; Canuto, S. Solvent Effects in Emission Spectroscopy: A Monte Carlo Quantum Mechanics Study of the N-Π* Shift of Formaldehyde in Water. *J. Chem. Phys.* **2000**, *113*, 9132−9139.
(52) Warshel, A.; Levitt, M. Theoretical Studies of Enzymic Reactions: Dielectric, Electrostatic and Steric Stabilization of the Carbonium Ion in the Reaction of Lysozyme. *J. Mol. Biol.* **1976**, *103*, 227−249.
(53) Field, M. J.; Bash, P. A.; Karplus, M. A Combined Quantum Mechanical and Molecular Mechanical Potential for Molecular Dynamics Simulations. *J. Comput. Chem.* **1990**, *11*, 700−733.
(54) Coutinho, K.; Canuto, S. *DICE, A Monte Carlo Program for Molecular Liquid Simulation*, Universidade de São Paulo, 2010.
(55) Jorgensen, W. L.; Chandrasekhar, J.; Madura, J. D.; Impey, R. W.; Klein, M. L. Comparison of Simple Potential Functions for Simulating Liquid Water. *J. Chem. Phys.* **1983**, *79*, 926−935.
(56) Jorgensen, W. L.; Maxwell, D. S.; Tirado-Rives, J. Development and Testing of the OPLS All-Atom Force Field on Conformational Energetics and Properties of Organic Liquids. *J. Am. Chem. Soc.* **1996**, *118*, 11225−11236.
(57) Breneman, C. M.; Wiberg, K. B. Determining Atom-Centered Monopoles from Molecular Electrostatic Potentials. The Need for High Sampling Density in Formamide Conformational Analysis. *J. Comput. Chem.* **1990**, *11*, 361−373.
(58) Coutinho, K.; Guedes, R. C.; Cabral, B. J. C.; Canuto, S. Electronic Polarization of Liquid Water: Converged Monte Carlo-Quantum Mechanics Results for the Multipole Moments. *Chem. Phys. Lett.* **2003**, *369*, 345−353.
(59) Stillinger, F. H.; Rahman, A. Molecular Dynamics Study of Temperature Effects on Water Structure and Kinetics. *J. Chem. Phys.* **1972**, *57*, 1281−1292.
(60) Mezei, M.; Beveridge, D. L. Theoretical Studies of Hydrogen Bonding in Liquid Water and Dilute Aqueous Solutions. *J. Chem. Phys.* **1981**, *74*, 622−632.
(61) Humphrey, W.; Dalke, A.; Schulten, K. VMD: Visual Molecular Dynamics. *J. Mol. Graph.* **1996**, *14*, 33−38.
(62) Diem, M.; Photos, E.; Khouri, H.; Nafie, L. A. Vibrational Circular Dichroism in Amino Acids and Peptides. 3. Solution- and Solid-Phase Spectra of Alanine and Serine. *J. Am. Chem. Soc.* **1979**, *101*, 6829−6837.
(63) Pople, J. A.; Scott, A. P.; Wong, M. W.; Radom, L. Scaling Factors for Obtaining Fundamental Vibrational Frequencies and Zero-Point Energies from HF/6-31G* and MP2/6-31G* Harmonic Frequencies. *Isr. J. Chem.* **1993**, *33*, 345−350.
(64) Wong, M. W. Vibrational Frequency Prediction Using Density Functional Theory. *Chem. Phys. Lett.* **1996**, *256*, 391−399.
(65) Diem, M. Infrared Vibrational Circular Dichroism of Alanine in the Midinfrared Region: Isotopic Effects. *J. Am. Chem. Soc.* **1988**, *110*, 6967−6970.